Electronic Supplementary Material (ESI) for Chemical Science.
This journal is © The Royal Society of Chemistry 2018

Supplementary Information

Supercooling of functional alkyl-π molecular liquids

Fengniu Lu,[a] Keumhee Jang,[a] Izabela Osica,[b] Keita Hagiwara,[c] Michito Yoshizawa,[c] Masashi Ishii,[d] Yoshiaki Chino,[e] Kazuchika Ohta,[e] Kinga Ludwichowska,[b] Krzysztof Jan Kurzydłowski,[b] Shinsuke Ishihara[a] and Takashi Nakanishi *[a]

a. International Center for Materials Nanoarchitectonics (WPI-MANA), National Institute for Materials Science (NIMS), 1-1 Namiki, Tsukuba 305-0044, Japan. E-mail: *nakanishi.takashi@nims.go.jp (T. Nakanishi)*

b. Materials Design Division, Faculty of Materials Science and Engineering, Warsaw University of Technology, Woloska 141, 02-507 Warsaw, Poland.

c. Laboratory for Chemistry and Life Science, Institute of Innovative Research, Tokyo Institute of Technology, 4259 Nagatsuta, Midori-ku, Yokohama 226-8503, Japan.

d. Materials Data Platform Center, Research and Services Division of Materials Data and Integrated System (MaDIS), NIMS, 1-2-1 Sengen, Tsukuba 305-0047, Japan.

e. Material Science and Technology, Interdisciplinary Graduate School of Science and Technology, Shinshu University, 1-15-1 Tokida, Ueda 386-8567, Japan

Table of Contents

Experimental Section

Materials

All starting materials and reagents, unless otherwise specified, were purchased from commercial suppliers (where noted) and used without further purification. 1-Bromo-2-ethylhexane (**BrC_2C_6**) was purchased from Tokyo Chemical Industry Co., Ltd. (TCI) and used as received. 1-Bromo-2-butyloctane (**BrC_4C_8**),[1] 1-Bromo-2-hexyl-decane (**BrC_6C_{10}**),[1,2] 1-bromo-2-decyl-tetradecane (**$BrC_{10}C_{14}$**),[2] and anthracene derivative **DPA8**[3] were synthesized and purified according to reported procedures. All reactions were performed under an argon atmosphere. Column chromatography was performed using silica gel 60 N (spherical, neutral, Kanto Chemical Co., Inc.). Spectroscopic grade solvents, dichloromethane (DOJINDO) and *n*-hexane (DOJINDO) were used for all spectroscopic studies without further purification.

Measurements

Recycling high performance liquid chromatography (HPLC) was performed at room temperature using a GPC column (YMC-GPC T30000 ϕ 20 × 600 mm) on a LC-9225NEXT system, equipped with RI and UV-Vis detectors. ^{1}H nuclear magnetic resonance (NMR) and ^{13}C NMR spectra were recorded on a *JEOL ECS-400* spectrometer at 400 MHz and 100 MHz, respectively, with tetramethylsilane used as the internal standard. Before ^{1}H and ^{13}C NMR measurements, all samples were dried up from their dichloromethane solution to check whether residual solvent remained or not. Matrix-assisted laser desorption ionization–time-of-flight mass spectra (MALDI-TOF MS) were obtained by a Shimadzu AXIMA-CFR Plus station.

Thermogravimetric analysis (TGA) was performed with a SII instrument TG/DTA 6200 or a TA instrument SDT Q600 (New Castle, DE, USA) under nitrogen flow at a heating rate of 10 °C min^{-1}. Differential scanning calorimetry (DSC) was measured using Hitachi High-Tech Science DSC7000X with liquid nitrogen cooling accessory under nitrogen flow at different scan rates (where noted). Optical micrographs were obtained under polarized and normal light conditions using an Olympus BX51 optical microscopy. The samples were sandwiched between two glass plates for both measurements. Small- and wide-angle X-ray scattering (SWAXS) measurements were performed using Anton Paar SAXSess mc^2 instrument. The samples were filled into quartz capillaries for measurements. Rheology experiments were carried out using an Anton Paar Physica MCR301 rheometer, using the parallel plate geometry (50 mm diameter) and a measuring sample thickness of 0.10 mm. For the measurement, strain amplitude scans were firstly performed to determine the linear-viscoelastic region and the strain amplitude of 0.002 was within this region.

For all optical absorption and fluorescence measurements, thin solvent-free liquid samples were sandwiched by two quartz plates and solid powder samples were prepared by grinding with barium sulphate ($BaSO_4$). UV-Vis absorption and fluorescence spectra in both solution and solvent-free liquid or solid state were recorded on a JASCO V-670 spectrophotometer and a JASCO FP-8300 spectrophotometer, respectively. The solid-state absorption spectra were obtained by Kubelka-Munk conversion. Absolute quantum yields were determined on a Hamamatsu Photonics absolute PL quantum yield spectrometer C11347. The temperature-dependent luminescence at low temperatures was measured from 10 °C to −110 °C by a monochromator with a 1200 lines/mm diffraction grating (JASCO CT-25S) and a CCD (TOSHIBA Corporation IK-627).

Synthesis and Characterization

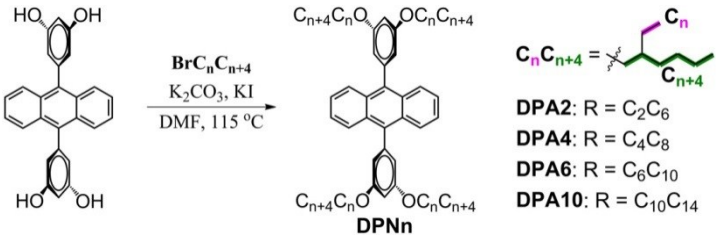

General synthetic procedure of DPAn (*n* = 2, 4, 6, and 10): A mixture of 9,10-bis(3,5-dihydroxyphenyl)anthracene (2.50 mmol; TCI), corresponding alkyl bromide **BrC_nC_{n+4}** (12.60 mmol), potassium carbonate (K_2CO_3, 20.30 mmol; TCI) and potassium iodide (KI, 0.50 mmol; Wako) in anhydrous DMF (30 mL) was refluxed at 115 °C for 20 h. The progress of the reaction was monitored by TLC. After the completion of the reaction, the reaction mixture was cooled to room temperature, excess chloroform was added and the mixture was washed with distilled water. The organic layer was washed with brine, dried over anhydrous sodium sulphate and the solvent was evaporated under reduced pressure. The purification was carried out by column chromatography (SiO_2, *n*-hexane/chloroform).

DPA2: white pasty solid (yield, 49%), m.p. 70–72 °C; TLC (SiO_2; $CHCl_3$:*n*-hexane, 95:5 v/v): R_f = 0.36; ^{1}H NMR (400 MHz, $CDCl_3$) δ (ppm): 7.80 (dd, J = 6.8, 3.2 Hz, 4H), 7.35 (dd, J = 6.8, 3.2 Hz, 4H), 6.65 (t, J = 2.0 Hz, 2H), 6.62 (d, J = 2.4 Hz, 4H), 3.86 (*d*, J = 5.6 Hz, 8H), 1.79–1.71 (*m*, 4H), 1.51–1.30 (*m*, 32H), 0.94–0.87 (*m*, 24H); ^{13}C NMR (100 MHz, $CDCl_3$) δ (ppm): 160.50, 140.90, 137.20, 129.54, 127.109, 124.96, 109.75, 100.85, 70.83, 39.45, 30.54, 29.09, 23.89, 23.05, 14.08, 11.14; MALDI-TOF MS (matrix: dithranol) calculated for $C_{58}H_{82}O_4$: 842.6, found: 842.4 $[M]^+$.

DPA4: white pasty solid (yield, 75%), m.p. 59–61 °C; TLC ($CHCl_3$:*n*-hexane, 95:5 v/v): R_f = 0.35; ^{1}H NMR (400 MHz, $CDCl_3$) δ (ppm): 7.80 (dd, J = 6.8, 3.2 Hz, 4H), 7.35 (dd, J = 6.8, 3.2 Hz, 4H), 6.64 (d, J = 2.0 Hz, 2H), 6.61 (t, J = 0.8 Hz, 4H), 3.85 (d, J = 5.6 Hz, 8H), 1.81–1.76 (*m*, 4H), 1.48–1.27 (*m*, 64H), 0.91–0.85 (*m*, 24H); ^{13}C NMR (100 MHz, $CDCl_3$) δ (ppm): 160.48, 140.89, 137.20, 129.54, 127.09, 124.95, 109.72, 100.85, 71.22, 38.00, 31.86, 31.41, 31.09, 29.70, 29.08, 26.83, 23.07, 22.68, 14.11; MALDI-TOF MS (matrix: dithranol) calculated for $C_{74}H_{114}O_4$: 1066.9, found: 1066.6 $[M]^+$.

DPA6: transparent yellowish liquid (yield, 57%); TLC ($CHCl_3$:*n*-hexane, 85:15 v/v): R_f = 0.37; ^{1}H NMR (400 MHz, $CDCl_3$) δ (ppm): 7.80 (dd, J = 6.8, 3.6 Hz, 4H), 7.35 (dd, J = 7.2, 3.2 Hz, 4H), 6.64 (t, J = 2.4 Hz, 2H), 6.61 (d, J = 2.0 Hz, 4H), 3.84 (d, J = 6.0 Hz, 8H), 1.80–1.76 (m, 4H), 1.47–1.26 (m, 96H), 0.88–0.85 (m, 24H); ^{13}C NMR (100 MHz, $CDCl_3$) δ (ppm): 160.49, 140.87, 137.20, 129.54, 127.09, 124.94, 109.74, 100.87, 71.25, 38.03, 31.90, 31.86, 31.41, 30.03, 29.69, 29.59, 29.33, 26.86, 26.83, 22.67, 14.11; MALDI-TOF MS (matrix: dithranol) calculated for $C_{90}H_{146}O_4$: 1291.1, found: 1290.9 $[M]^+$.

DPA10: transparent yellowish fluid (yield, 54%); TLC ($CHCl_3$:*n*-hexane, 90:10 v/v): R_f = 0.42; ^{1}H NMR (400 MHz, $CDCl_3$) δ (ppm): 7.80 (dd, J = 6.8, 3.2 Hz, 4H), 7.35 (dd, J = 6.8, 3.2 Hz, 4H), 6.64 (t, J = 2.0 Hz, 2H), 6.60 (t, J = 2.0 Hz, 4H), 3.84 (d, J = 6.0 Hz, 8H), 1.80–1.76 (m, 4H), 1.47–1.33 (m, 160H), 0.87 (td, J = 6.4, 1.6 Hz, 24H); ^{13}C NMR (100 MHz, $CDCl_3$) δ (ppm): 160.48, 140.86, 137.19, 129.53, 127.08, 124.93, 109.71, 100.80, 71.21, 38.03, 31.92, 31.38, 30.04, 29.69, 29.65, 29.36, 26.87, 22.69, 14.13; MALDI-TOF MS (matrix: dithranol) calculated for $C_{122}H_{210}O_4$: 1739.6, found 1740.3 $[M]^+$.

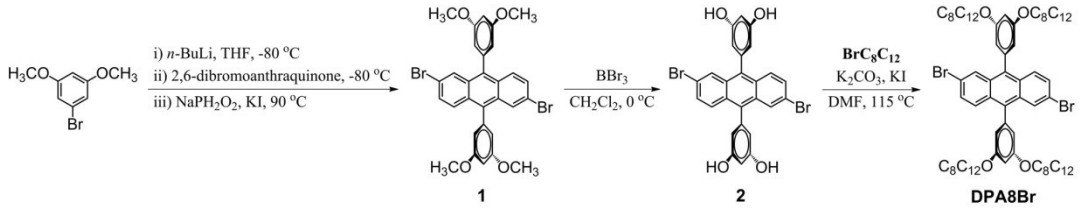

Synthesis of 1: To a solution of 1-bromo-3,5-dimethoxybenzene (14.31 g, 65.93 mmol; TCI) in 200 mL anhydrous THF at −80 °C under argon, *n*-butyllithium (*n*-BuLi, 24.7 mL, 64.30 mmol; 2.6 M in *n*-hexane, Kanto Chemical Co., Inc.) was carefully injected. The mixture was stirred for 1 h and a solution of 2,6-dibromoanthraquinone (4.81 g, 13.14 mmol; Sigma-Aldrich) in anhydrous THF (100 mL) was added. The mixture was further stirred for 1 h at −80 °C, and then warmed to room temperature. After the completion of the reaction, distilled water was added and the reaction mixture was extracted with ethyl acetate. The solvent was removed under reduced pressure. A mixture of the resultant solid, sodium hypophosphite ($NaPH_2O_2$, 8.77 g, 99.68 mmol; Alfa Aesar) and potassium iodide (KI, 4.38 g, 26.39 mmol; Wako) in acetic acid (150 mL; Kanto Chemical Co., Inc.) was stirred at 90 °C for 18 h. After the completion of the reaction, the reaction mixture was cooled to room temperature, excess chloroform was added and the mixture was washed with distilled water. The organic layer was washed with brine, dried over anhydrous sodium sulphate and the solvent was evaporated under reduced pressure. The purification carried out by column chromatography (SiO_2, *n*-hexane/ethyl acetate) yielded **1** as a yellow solid (4.69 g, 7.71 mmol).

1: yellow solid (yield, 59%); TLC (*n*-hexane:ethyl acetate, 10:1 v/v): R_f = 0.40; ^{1}H NMR (400 MHz, $CDCl_3$) δ (ppm): 7.88 (d, J = 1.8 Hz, 2H), 7.60 (d, J = 9.6 Hz, 2H), 7.39 (dd, J = 9.6, 1.6 Hz, 2H), 6.67 (d, J = 1.6 Hz, 2H), 6.57 (d, J = 1.6 Hz, 4H), 3.85 (s, 12H); MALDI-TOF MS (matrix: dithranol) calculated for $C_{30}H_{24}Br_2O_4$: 608.0, found: 608.5 $[M]^+$.

Synthesis of 2: To a solution of **1** (4.00 g, 6.58 mmol) in 150 mL anhydrous dichloromethane at 0 °C, boron tribromide (BBr_3, 60.0 mL, 60.00 mmol; 1.0 M in dichloromethane, TCI) was carefully added. The mixture was stirred for 17 h at room temperature under argon. After the completion of the reaction, the reaction mixture was washed with distilled water. The organic layer was washed with brine, dried over anhydrous sodium sulphate and the solvent was evaporated under reduce pressure. The purification carried out by column chromatography (SiO_2, *n*-hexane/ethyl acetate) gave **2** as a yellow solid (2.93 g, 5.30 mmol).

2: yellow solid (yield, 81%); TLC ($CHCl_3$:ethyl acetate, 1:1 v/v): R_f = 0.48; ^{1}H NMR (400 MHz, MeOH) δ (ppm): 7.89 (d, J = 2.0 Hz, 2H), 7.69 (d, J = 9.2 Hz, 2H), 7.45 (dd, J = 9.2, 2.0 Hz, 2H), 6.51 (d, J = 2.0 Hz, 2H), 6.35 (d, J = 2.0 Hz, 4H); MALDI-TOF MS (matrix: dithranol) calculated for $C_{26}H_{16}Br_2O_4$: 551.9, found: 552.1 $[M]^+$.

Synthesis of DPA8Br: A mixture of **2** (1.00 g, 1.81 mmol), 2-octhyldodecyloxy bromide (**BrC_8C_{12}**, 5.25 g, 14.53 mmol), potassium carbonate (K_2CO_3, 7.30 g, 52.82 mmol; TCI) in anhydrous dimethylformamide (DMF, 60 mL; Kanto Chemical Co., Inc.) was stirred at 115 °C for 48 h. After completion of the reaction, the reaction mixture was cooled to room temperature, excess chloroform was added and washed with distilled water. The organic layer was washed with brine, dried over anhydrous sodium sulphate, and the solvent was evaporated under reduced pressure. The crude product was purified via column chromatography (SiO_2, *n*-hexane/chloroform) and subsequent recycling HPLC with chloroform as the solvent to give **DPA8Br** (2.31 g, 1.38 mmol) as a yellow liquid.

DPA8Br: yellow liquid (yield, 76%); TLC (*n*-hexane): R_f = 0.75; ^{1}H NMR (400 MHz, $CDCl_3$) δ (ppm): 7.92 (d, J = 2.0 Hz, 2H), 7.64 (d, J = 9.2 Hz, 2H), 7.38 (dd, J = 9.2, 2.0 Hz, 2H), 6.65 (t, J = 2.0 Hz, 2H),

6.53 (d, J = 2.4 Hz, 4H), 3.86 (d, J = 5.6 Hz, 8H), 1.81-1.77 (m, 4H), 1.48–1.25 (m, 128H), 0.87 (t, J = 6.4 Hz, 24H); ^{13}C NMR (100 MHz, $CDCl_3$) δ (ppm): 160.65, 139.44, 136.89, 130.52, 129.11, 129.04, 128.74, 128.48, 120.15, 109.59, 101.15, 71.28, 38.03, 31.91, 31.39, 30.04, 29.93, 29.68, 29.65, 29.61, 29.35, 26.89, 22.68, 14.12; MALDI-TOF MS (matrix: dithranol) calculated for $C_{106}H_{176}Br_2O_4$: 1671.2, found: 1672.7 $[M+H]^+$.

NMR spectra and MALDI-TOF MS

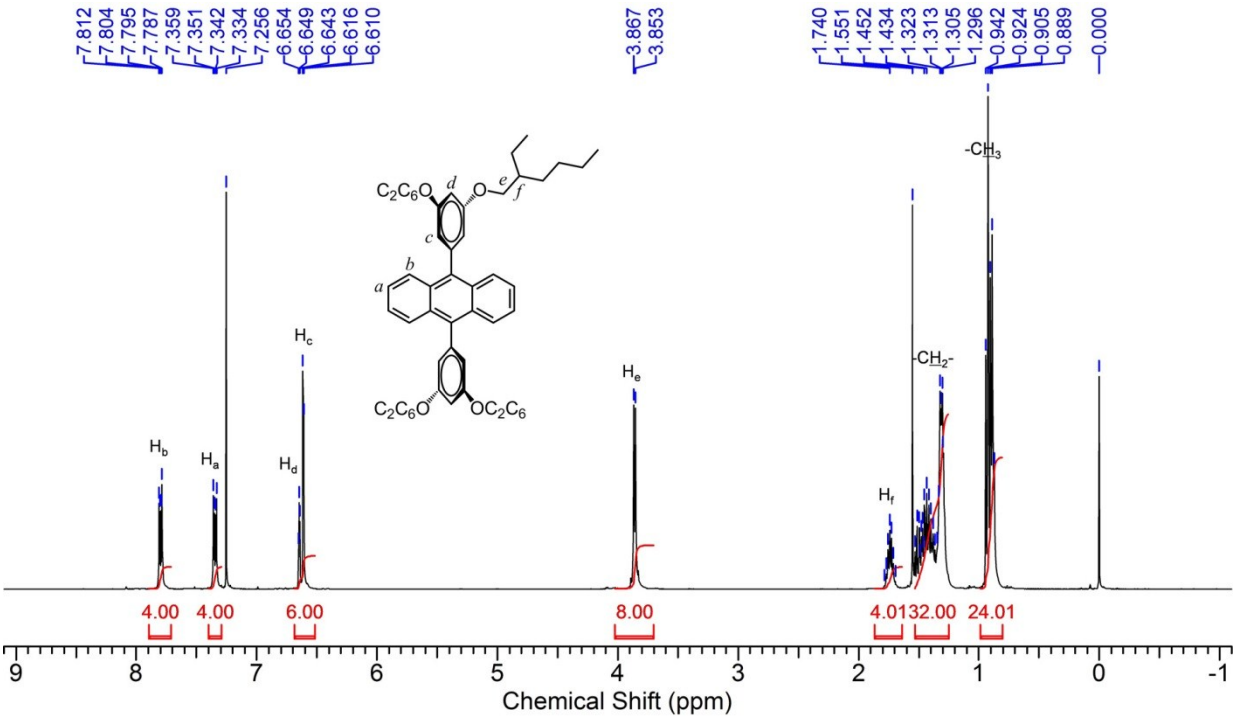

^{1}H NMR (400 MHz, $CDCl_3$) spectrum of **DPA2**.

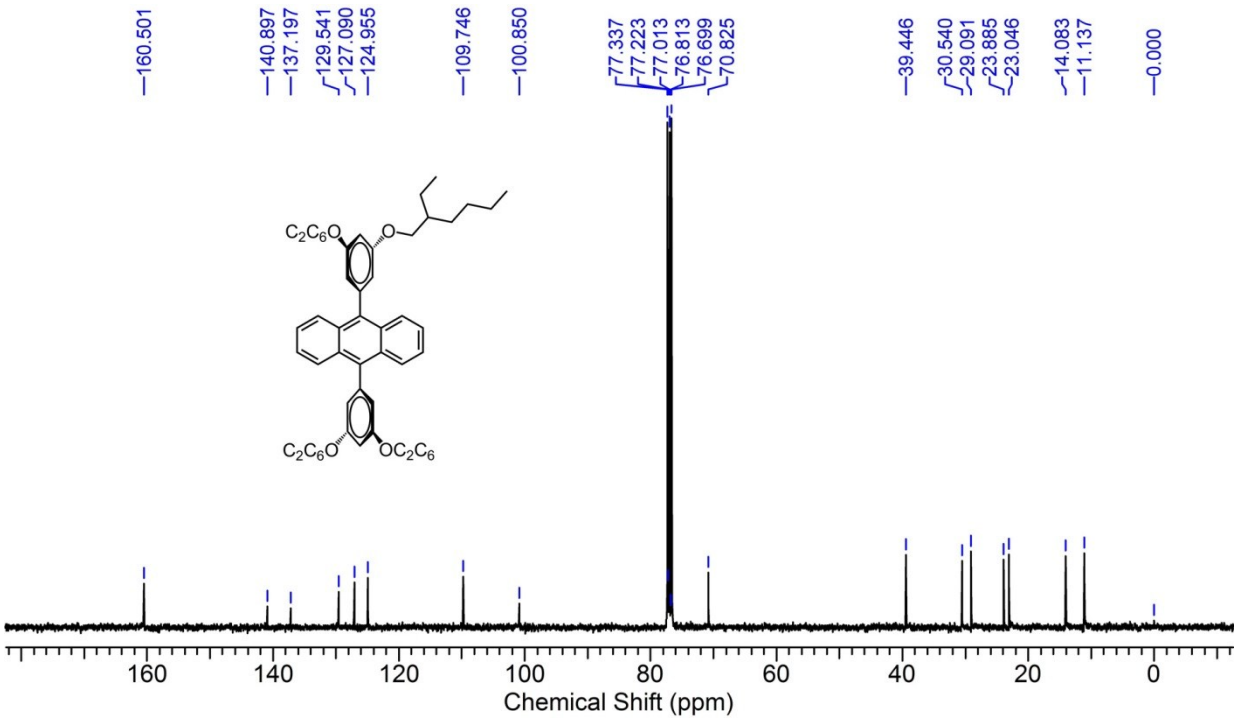

^{13}C NMR (100 MHz, $CDCl_3$) spectrum of **DPA2**.

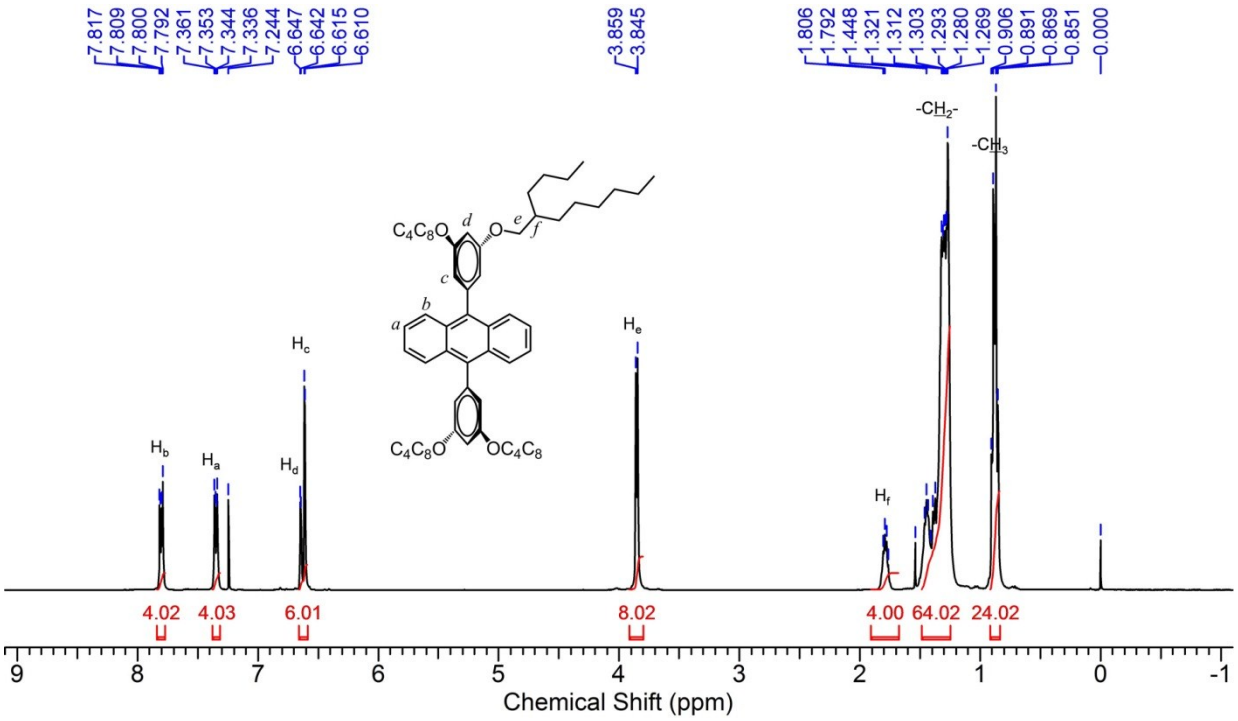

^{1}H NMR (400 MHz, $CDCl_3$) spectrum of **DPA4**.

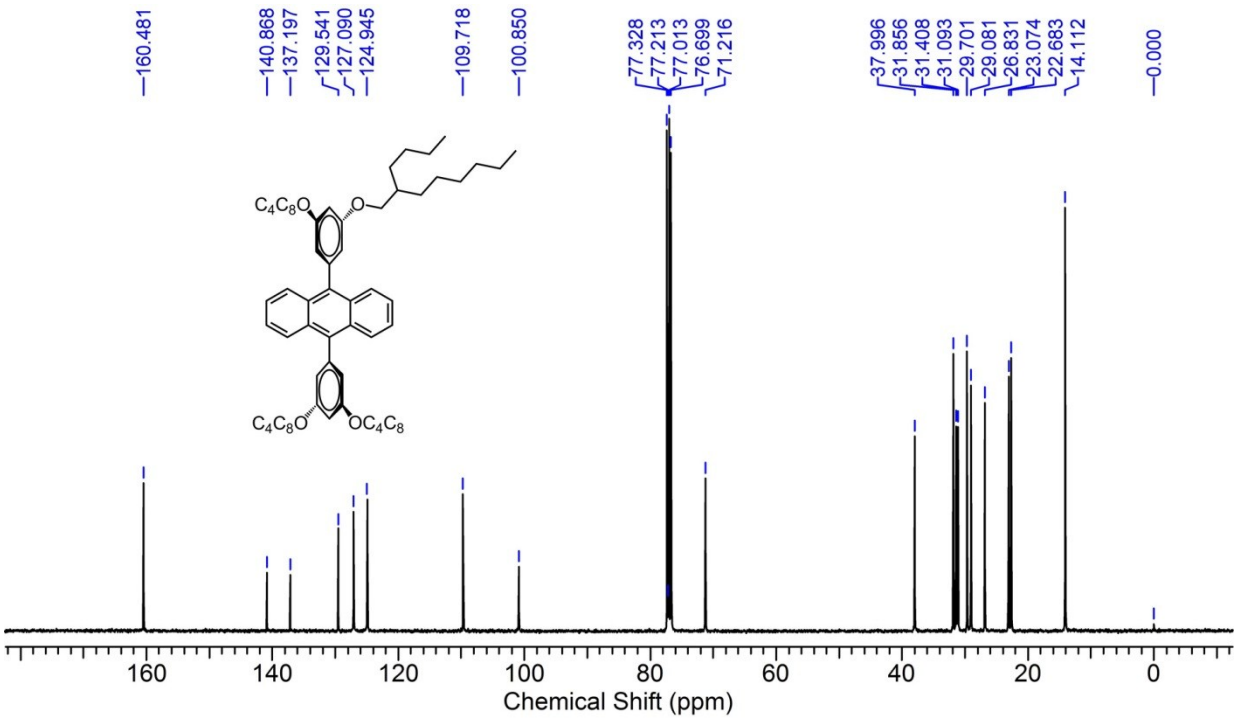

^{13}C NMR (100 MHz, $CDCl_3$) spectrum of **DPA4**.

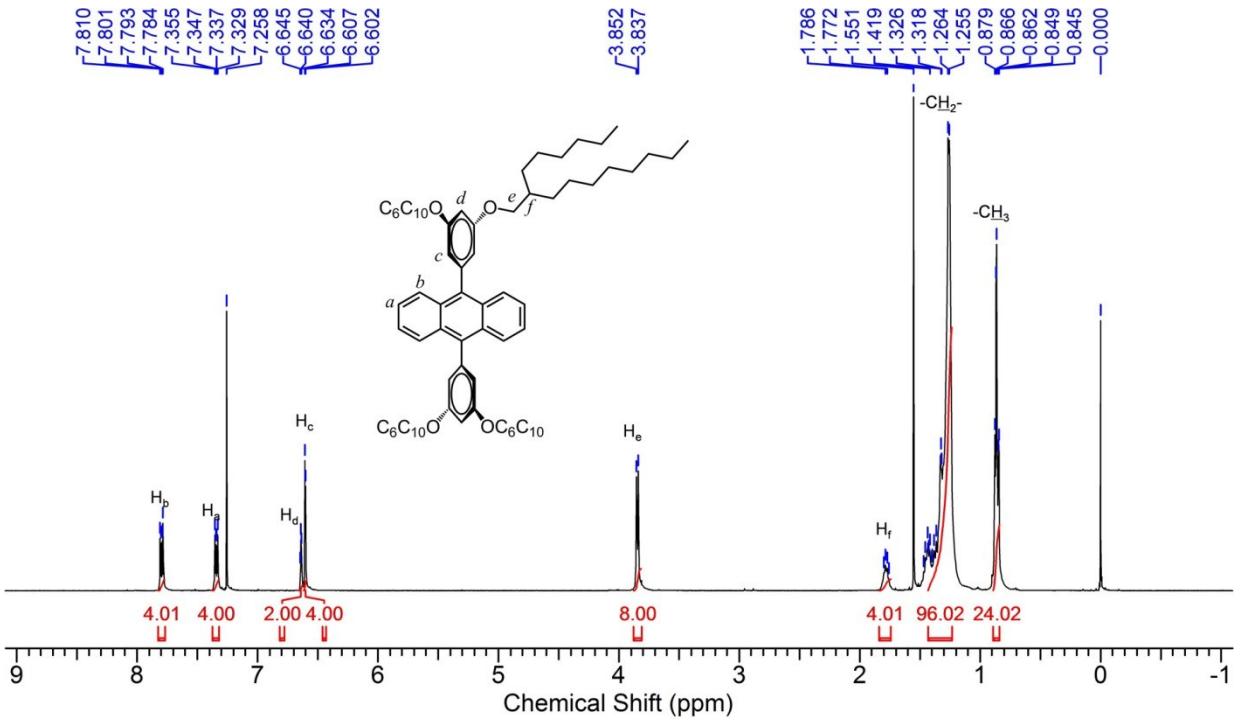

^{1}H NMR (400 MHz, $CDCl_3$) spectrum of **DPA6**.

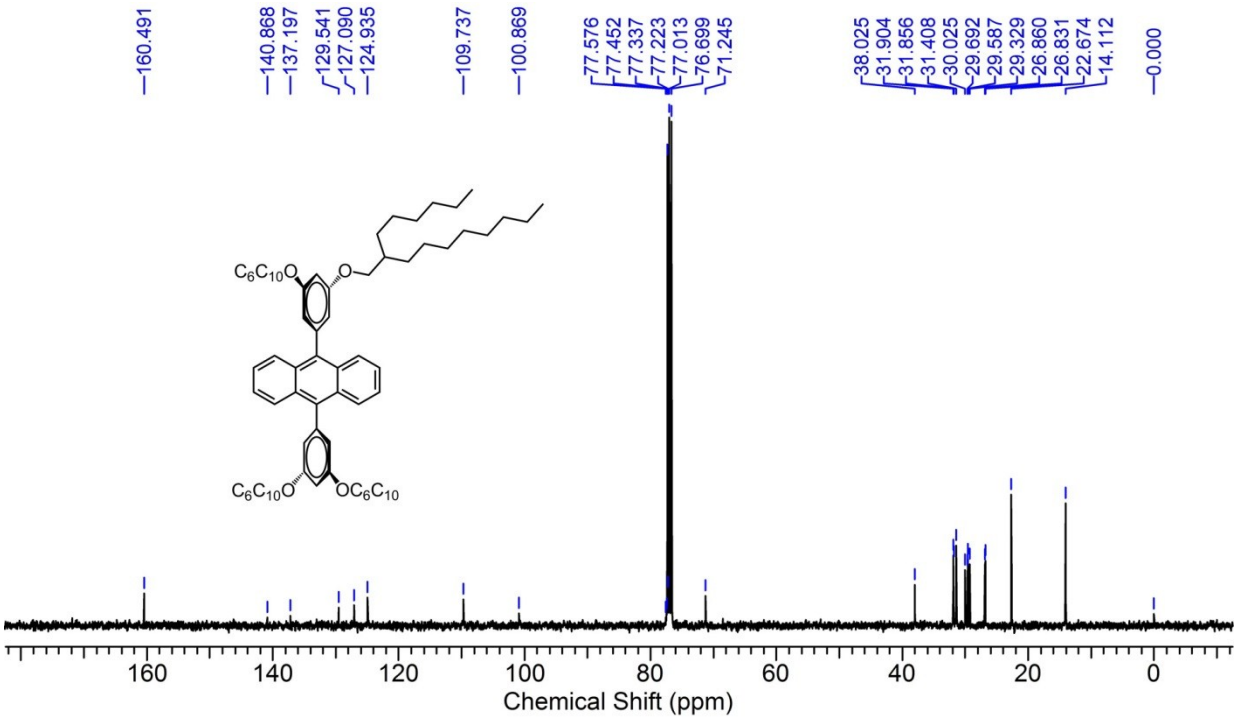

^{13}C NMR (100 MHz, $CDCl_3$) spectrum of **DPA6**.

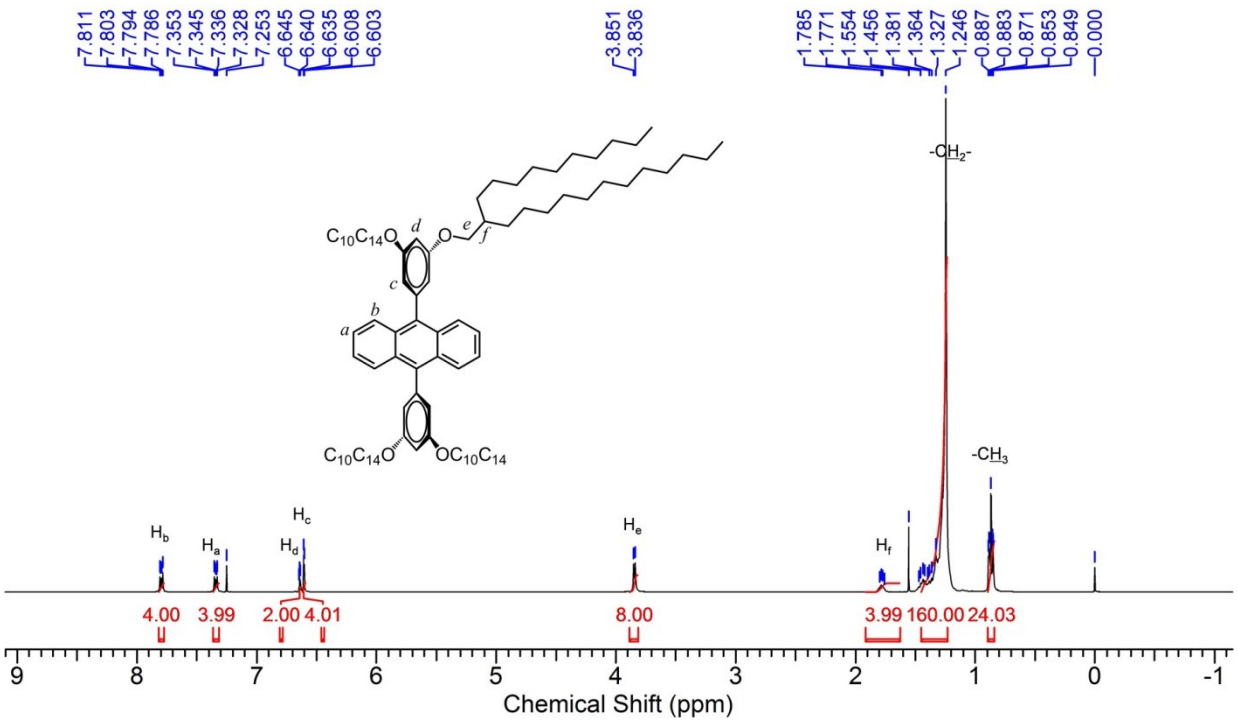

^{1}H NMR (400 MHz, $CDCl_3$) spectrum of **DPA10**.

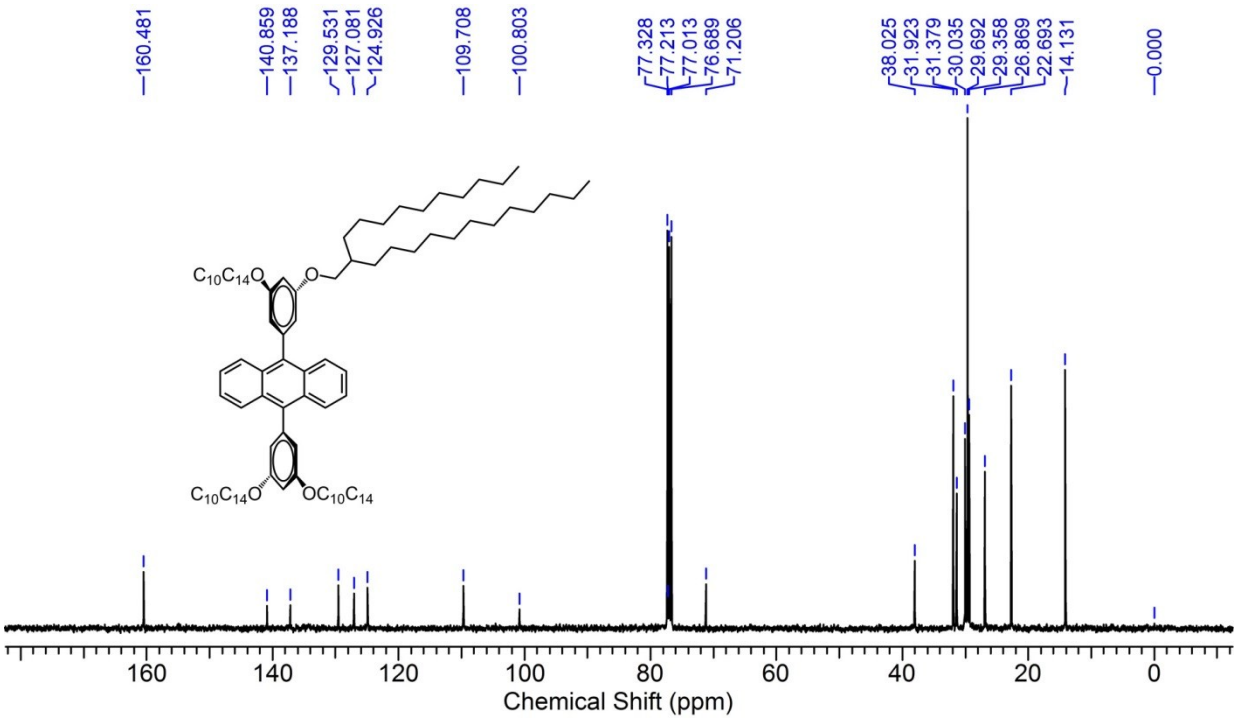

^{13}C NMR (100 MHz, $CDCl_3$) spectrum of **DPA10**.

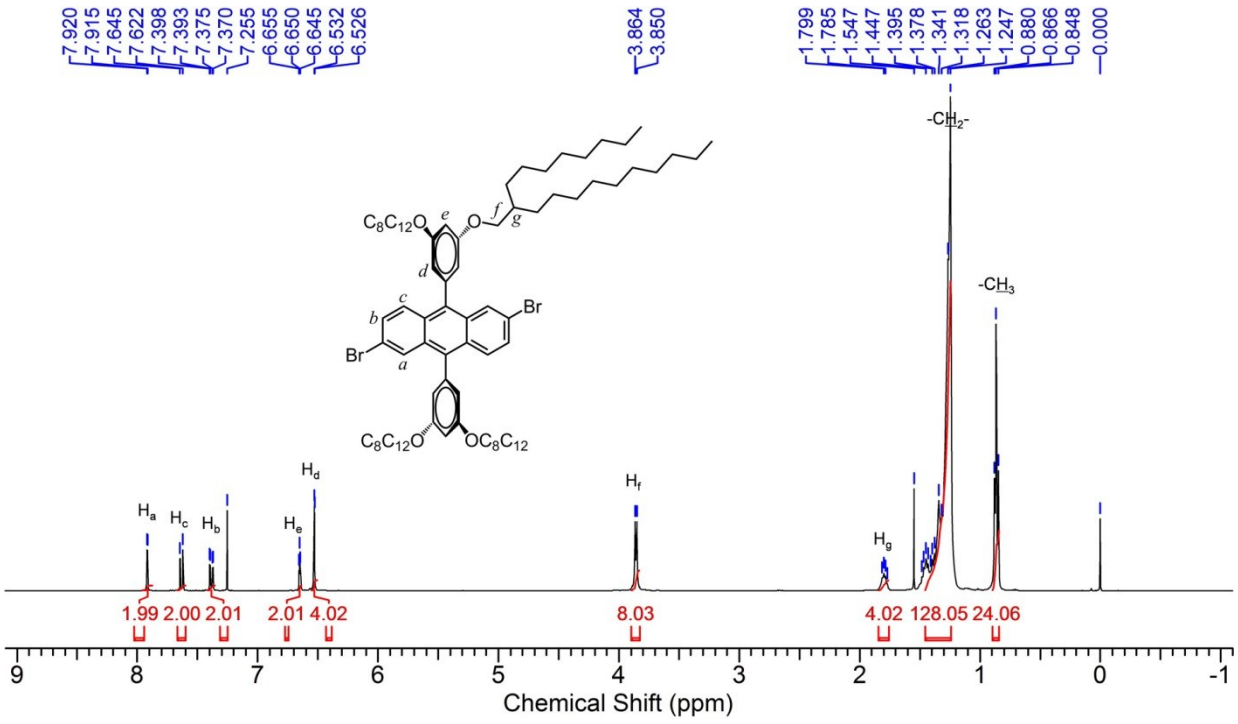

^{1}H NMR (400 MHz, $CDCl_3$) spectrum of **DPA8Br**.

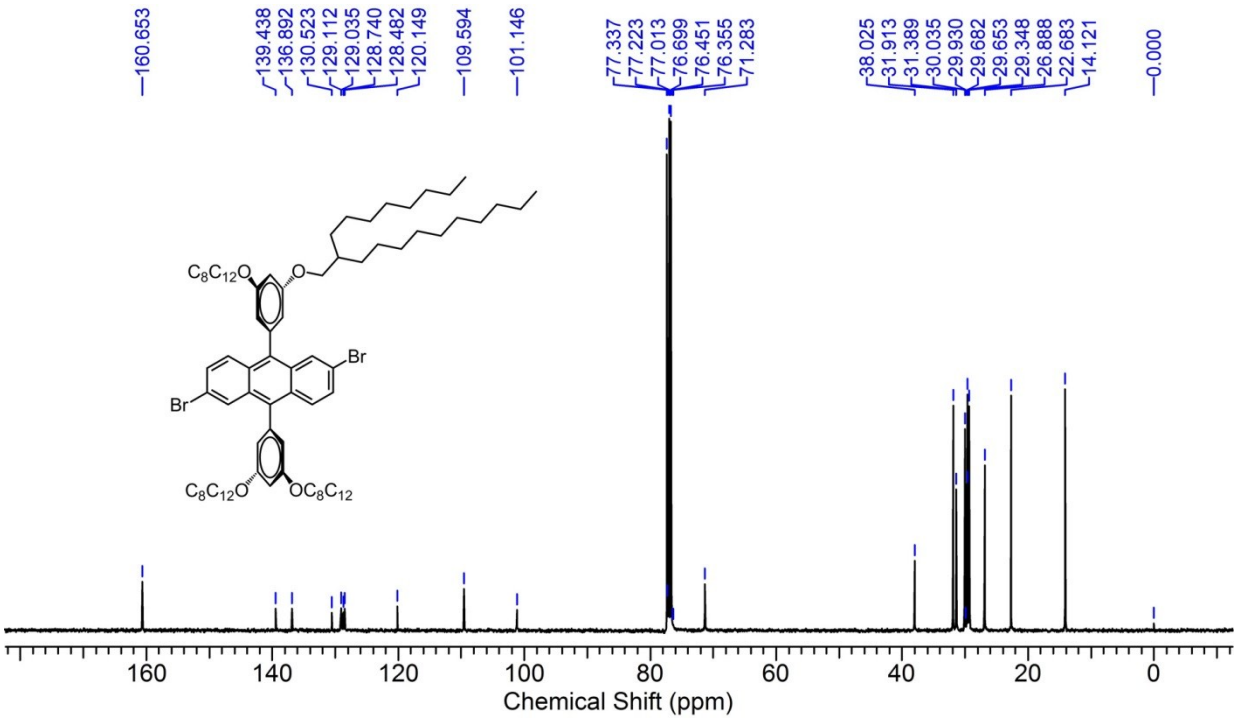

^{13}C NMR (100 MHz, $CDCl_3$) spectrum of **DPA8Br**.

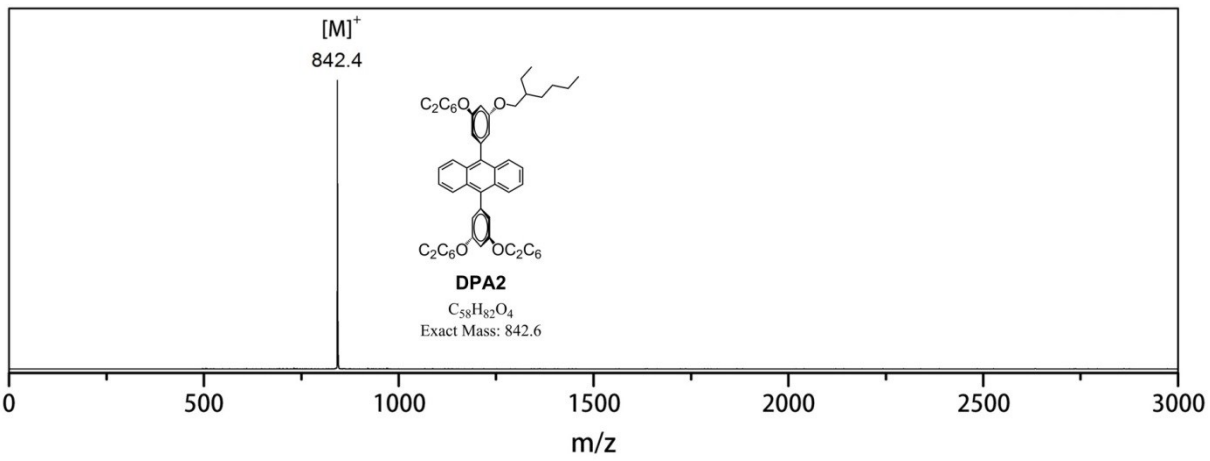

MALDI-TOF MS of **DPA2**. Matrix: dithranol.

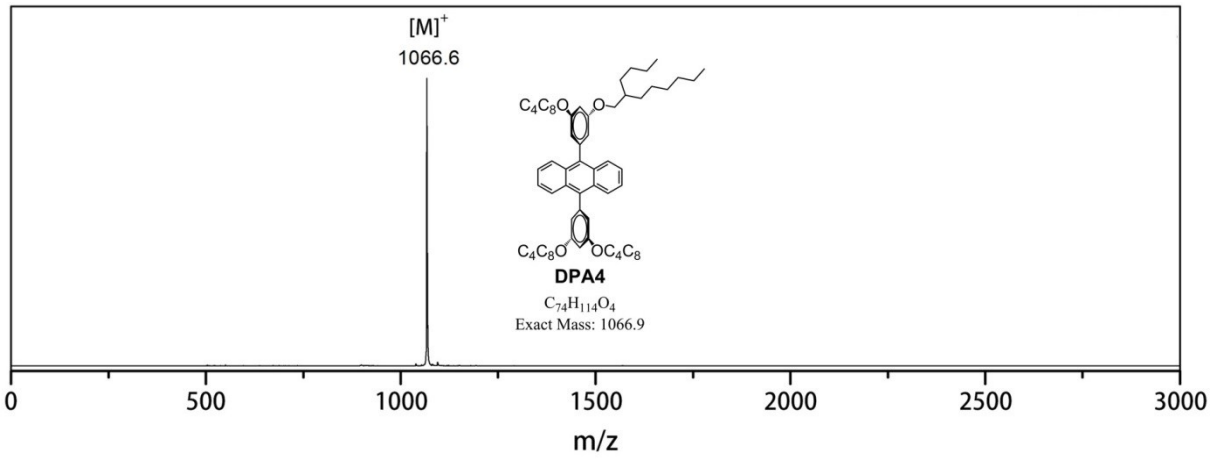

MALDI-TOF MS of **DPA4**. Matrix: dithranol.

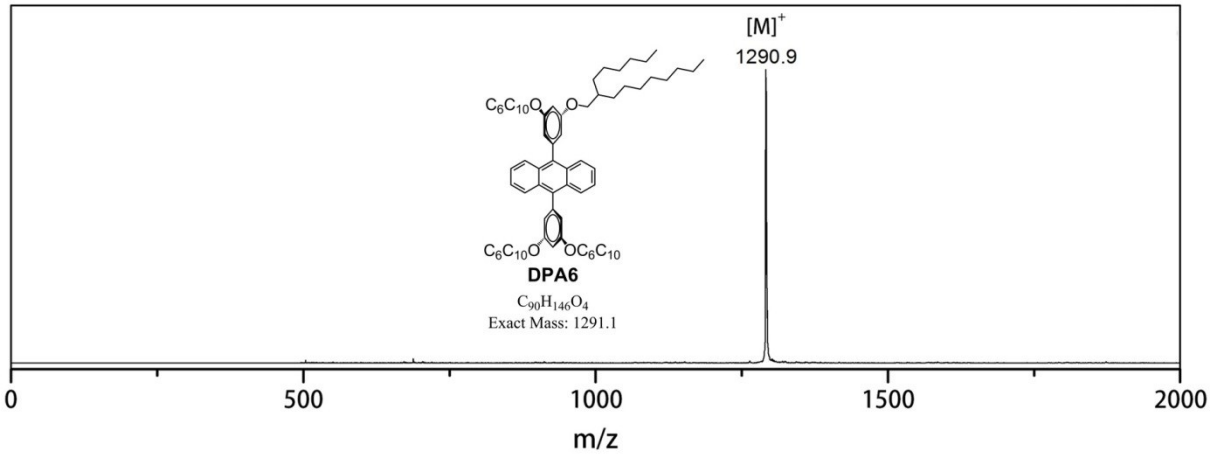

MALDI-TOF MS of **DPA6**. Matrix: dithranol.

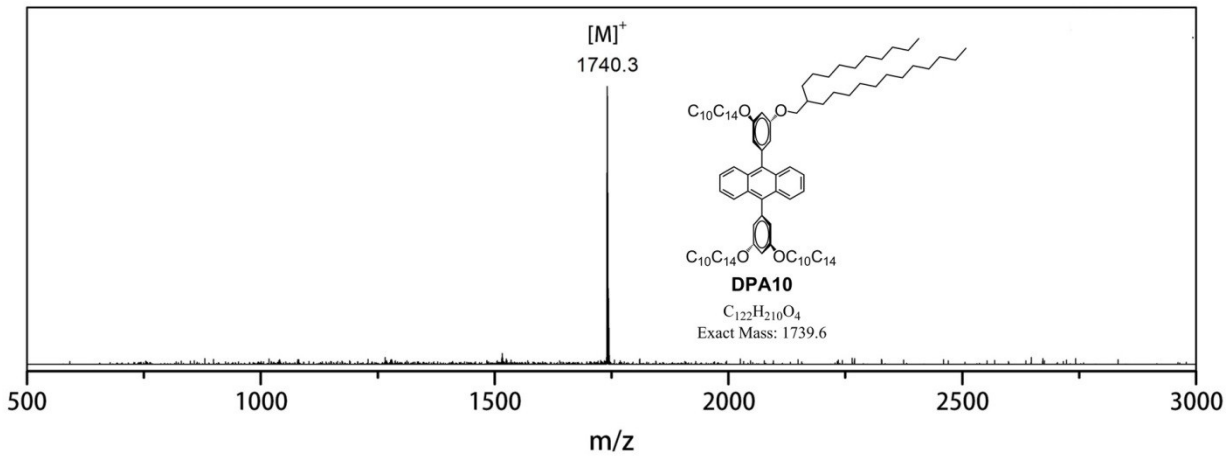

MALDI-TOF MS of **DPA10**. Matrix: dithranol.

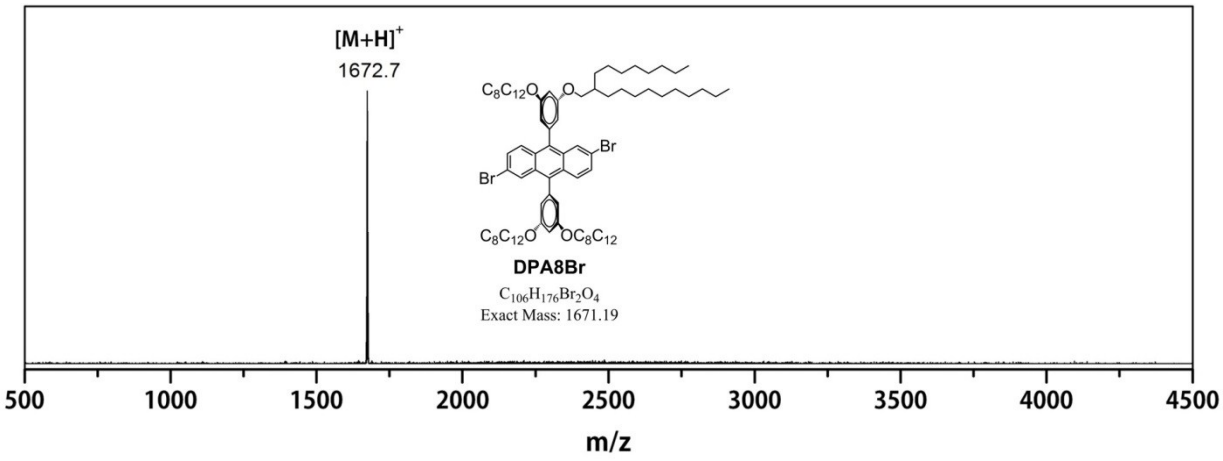

MALDI-TOF MS of **DPA8Br**. Matrix: dithranol.

2. Supplementary Figures

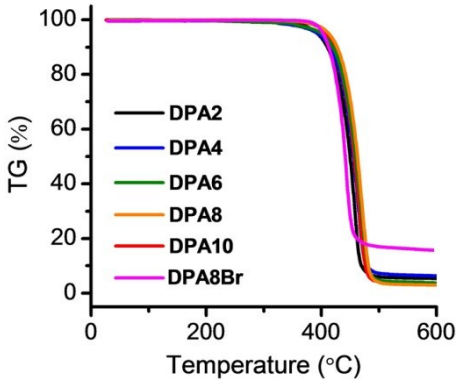

Figure S1. Thermogravimetric analysis of **DPAn**. The mass loss% at 300 °C were calculated as 0.18% (**DPA2**), 0.74% (**DPA4**), 0.96% (**DPA6**), 0.05% (**DPA8**), 0.35% (**DPA10**), and 0.s05% (**DPA8Br**).

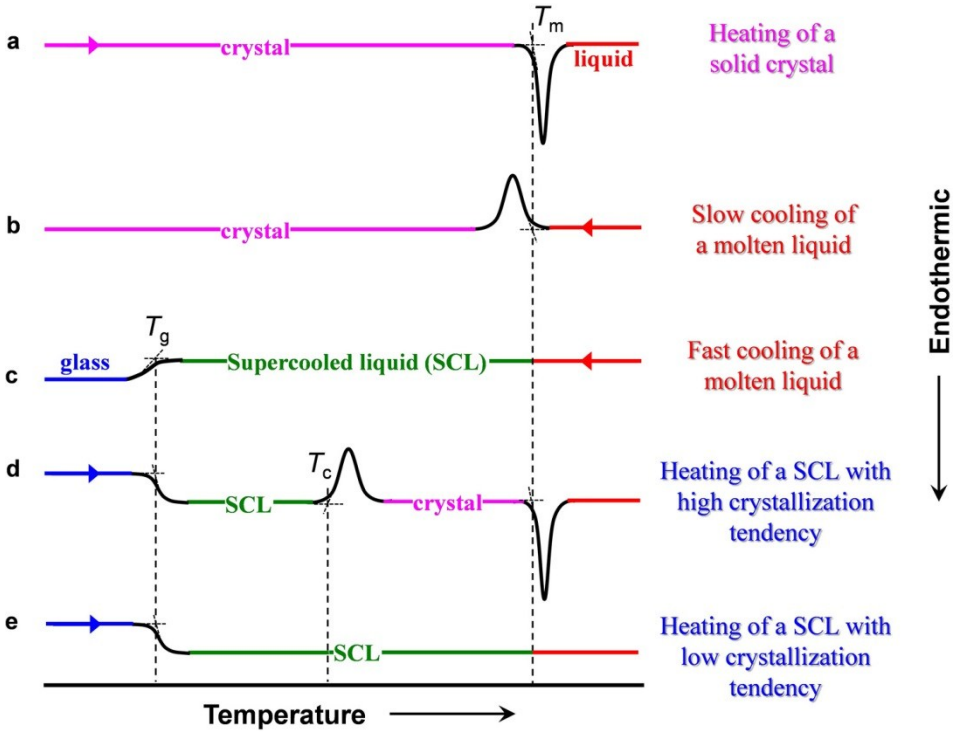

Figure S2. Schematic DSC thermograms of typical organic crystals (Adapted from ref [6]). (**a**) Heating of a solid crystal which melts into liquid above the melting point (T_m). (**b**) Slow cooling of a molten liquid which crystallizes into solid below the T_m. (**c**) Rapid cooling of a molten liquid which remains as supercooled liquid (SCL) below the T_m and turns into glass below the T_g. (**d**) Heating of a glass which turns into SCL above the T_g; the SCL crystallizes at the crystalline temperature (T_c) and then melts above the T_m. (**e**) Heating of a glass which turns into SCL above the T_g and remains as liquid; the time scale of the measurement is not long enough for the SCL to crystallize.

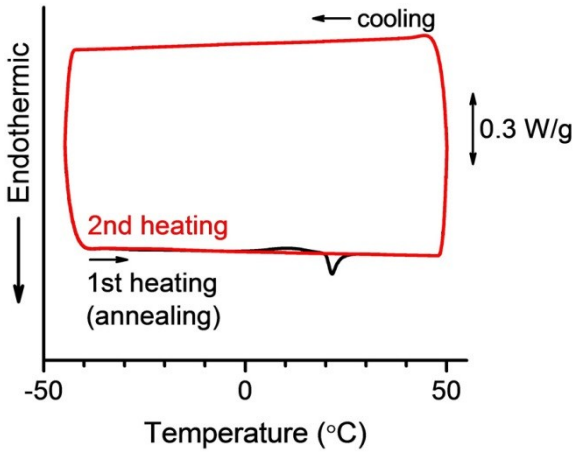

Figure S3. DSC thermograms of **DPA8** in the heating/cooling cycles (black line, 1st cycle; red line, 2nd cycle) between −45 and 45 °C at 10 °C min^{-1} under nitrogen flow; the sample was annealed at −45 °C for 12 hours before the 1st heating only.

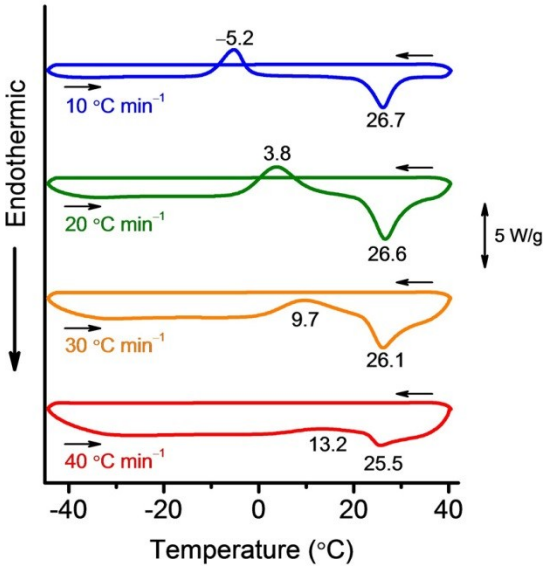

Figure S4. DSC diagrams of **DPA10** during the heating/cooling cycles between −45 and 40 °C at 10 °C min^{-1} (blue line), 20 °C min^{-1} (green line), 30 °C min^{-1} (orange line), and 40 °C min^{-1} (red line) under nitrogen flow. The crystallization and melting temperatures (°C) were denoted inside.

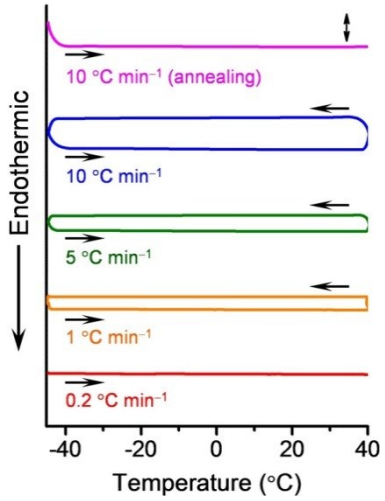

Figure S5. DSC thermograms of **DPA6** during the heating scan from −45 to 40 °C at 10 °C min^{-1} after annealing at −45 °C for 12 hours (magenta line; scale bar, 0.5 W/g), and during the heating/cooling cycles between −45 and −40 °C at 10 °C min^{-1} (blue line; scale bar, 1 W/g), 5 °C min^{-1} (green line; scale bar, 1 W/g), 1 °C min^{-1} (orange line; scale bar, 0.25 W/g), and 0.2 °C min^{-1} (red line; scale bar, 0.25 W/g) under nitrogen flow.

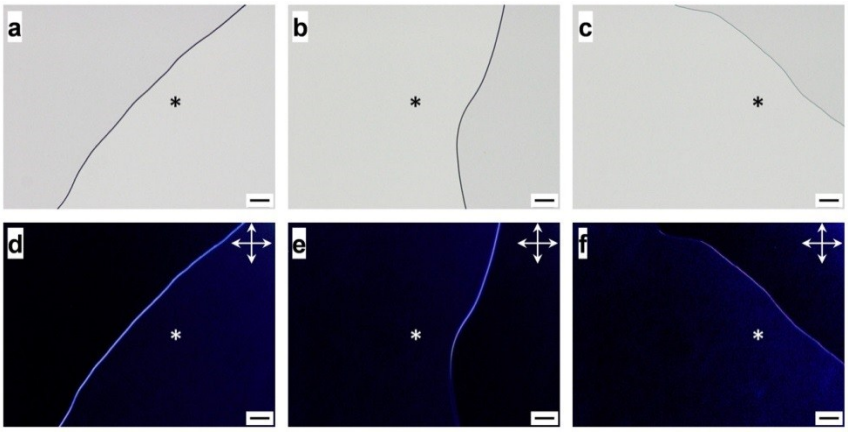

Figure S6. Optical (up) and polarized optical (below) micrographs of **DPA6** (**a** and **d**), **DPA8** (**b** and **e**), and **DPA10** (**c** and **f**) taken at 30 °C. The sample area was denoted with asterisk (∗). Scale bar, 50 μm.

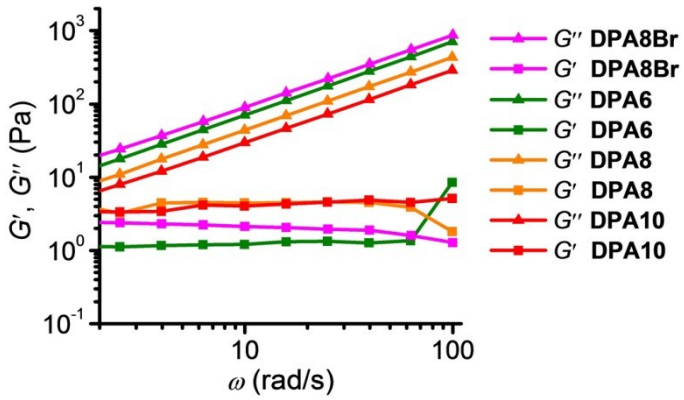

Figure S7. Storage elastic modulus (G', squares) and viscous loss modulus (G'', triangles) of **DPA6** (green), **DPA8** (orange), **DPA10** (red), and **DPA8Br** (magenta) as a function of angular frequency (ω) at 30 °C.

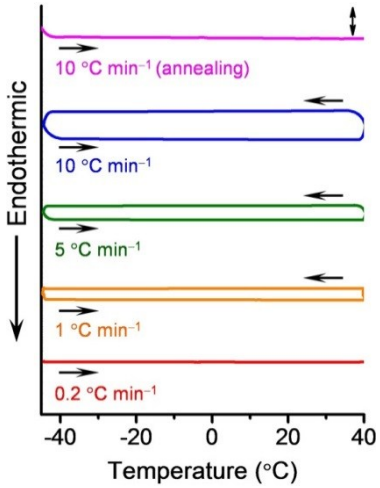

Figure S8. DSC thermograms of **DPA8Br** during the heating scan from −45 to 40 °C at 10 °C min^{-1} after annealing at −45 °C for 12 hours (magenta line; scale bar, 0.25 W/g), and during the heating/cooling cycles between −45 and 40 °C at 10 °C min^{-1} (blue line; scale bar, 1 W/g), 5 °C min^{-1} (green line; scale bar, 1 W/g), 1 °C min^{-1} (orange line; scale bar, 0.25 W/g), and 0.2 °C min^{-1} (red line; scale bar, 0.25 W/g) under nitrogen flow.

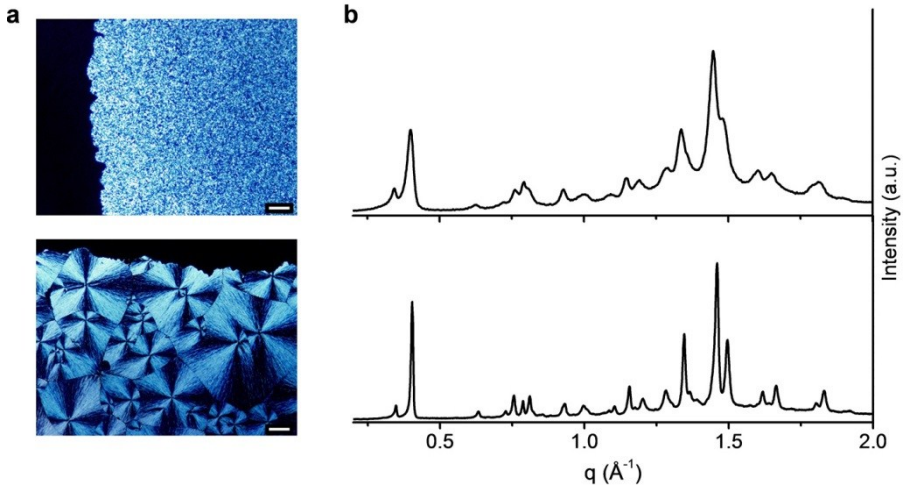

Figure S9. (**a**) Polarized optical micrographs of **DPA10** at 15 °C upon heating from −30 °C at 10 °C min^{-1} (up) and at −5 °C after aging at −5 °C for 7 hours (below). Scale bar, 50 μm. (**b**) SWAXS profiles of **DPA10** at 15 °C by heating up from −30 °C at 10 °C min^{-1} (up) and at −5 °C after aging at −5 °C for 7 days (below).

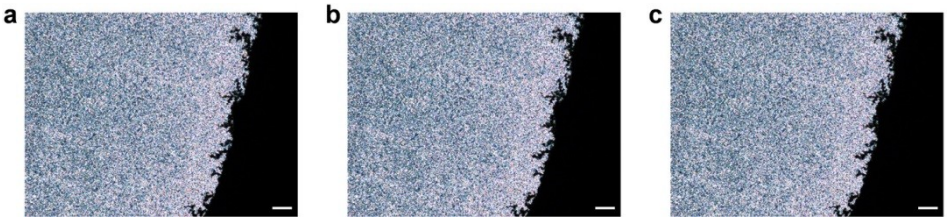

Figure S10. Polarized optical micrographs of **DPA10** at 15 °C before (**a**) and after pressing (**b**) and shearing (**c**). Scale bar, 100 μm.

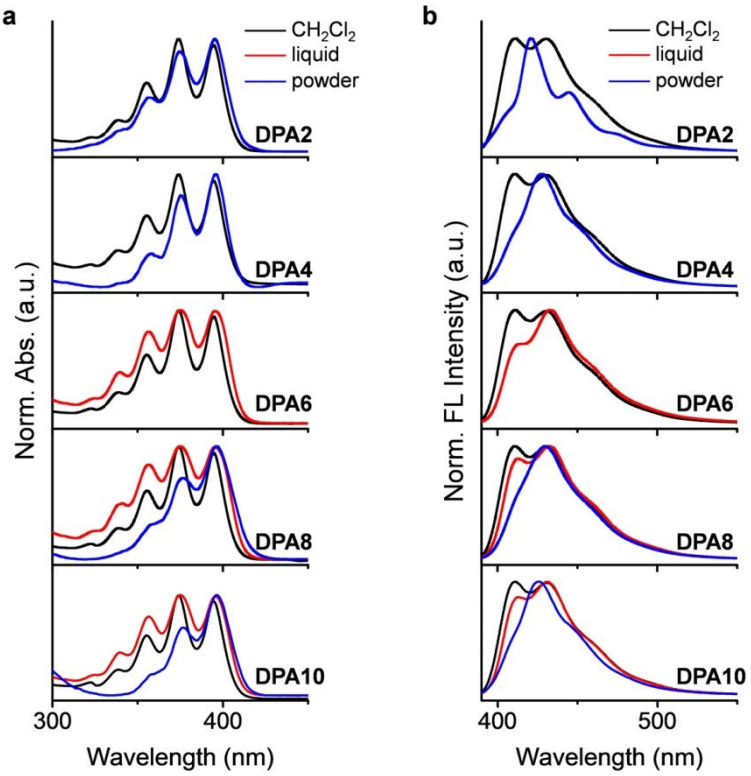

Figure S11. Normalized UV-vis absorption (**a**) and fluorescence (**b**) spectra of **DPA2**, **DPA4**, **DPA6**, **DPA8**, and **DPA10** (as denoted inside) in diluted CH_2Cl_2 solution (10^{-5} M, black line) and solvent-free solid (blue line) or liquid (red line) state**.** λ_{ex} = 374 nm. The different vibronic structures of the fluorescence band between the dichloromethane (CH_2Cl_2) solutions and the liquids were due to different media surrounding the chromophores, *i.e.*, CH_2Cl_2 in the solutions and chromophore molecules in the liquids.

Supplementary Figures

Table S1. Physical characteristics ($T_{g,\,offset}$: the offset temperature of glass transition in the 1st heating trace; T_m: melting point; ΔH: enthalpy; ΔS: entropy; $T_{d95\%}$: decomposition temperature; and η^*: complex viscosity) of **DPAn** and **DPA8Br**.

Compound	$T_{g,\,offset}$ (°C)[a]	T_m (°C)[b]	ΔH (kJ mol^{-1})	ΔS (J mol^{-1} K^{-1})	$T_{d95\%}$ (°C)[d]	η^* (Pa·s)[e]
DPA2	—	71.0	45.4	131.8[c]	393	—
DPA4	—	60.5	37.0	111.0[c]	394	—
DPA6	−51.1	—	—	—[c]	400	7.1
DPA8	−57.7	21.6	2.1	7.0	413	4.4
DPA10	−50.1	26.7	140.3	468.0	405	3.0
DPA8Br	−50.8	—	—	—	406	9.0

[a] Determined in the first DSC heating scan at 10 °C min^{-1} under N_2.
[b] Determined in the first DSC heating scan at 10 °C min^{-1} under N_2.
[c] **DPA8** was annealed at −45 °C for 12 hours before heating.
[d] Determined at 5% weight loss on TGA.
[e] Determined at angular frequency (ω) = 10 rad s^{-1} at 30 °C.

Table S2. Photophysical parameters (λ: wavelength; ε: absorption coefficient; and Φ_{FL}: absolute fluorescence quantum yield) of **DPAn** in CH_2Cl_2 solution (10^{-5} M) and solvent-free fluid or solid state.

Compound	Absorption Feature λ_{abs}, nm (ε, 10^4 dm^3 mol^{-1} cm^{-1})			Fluorescence λ_{max}, nm (Φ_{FL})			CIE (x, y)		
	CH_2Cl_2	Fluid[a]	Solid	CH_2Cl_2	Fluid[a]	Solid	CH_2Cl_2	Fluid[a]	Solid
DPA2	355 (1.57) 374 (2.57) 395 (2.43)	—	358 375 395	412 (0.85)	—	421 (0.58)	0.16, 0.04	—	0.16, 0.04
DPA4	355 (1.60) 374 (2.53) 395 (2.38)	—	358 375 396	411 (0.84)	—	427 (0.71)	0.16, 0.04	—	0.16, 0.04
DPA6	355 (1.34) 374 (2.21) 395 (2.09)	357 375 396	—	411 (0.84)	433 (0.49)	—	0.16, 0.04	0.16, 0.06	—
DPA8	355 (0.87) 374 (1.44) 395 (1.36)	355 374 395	376 396	411 (0.82)	432 (0.52)	430 (0.60)	0.16, 0.04	0.15, 0.05	0.16, 0.04
DPA10	355 (0.98) 374 (1.64) 394 (1.54)	355 374 394	376 396	411 (0.84)	431 (0.62)	425 (0.68)	0.16, 0.04	0.16, 0.05	0.16, 0.04
DPA8Br	364 (1.32) 383 (1.74) 404 (1.78)	364 383 404	—	420 (0.47)	444 (0.37)	—	0.16, 0.05	0.15, 0.08	—

[a] Prepared by sandwiching the fluid between two quartz plates.

References

1 B. Tylleman, G. Gbabode, C. Amato, C. Buess-Herman, V. Lemaur, J. Cornil, R. Gómez Aspe, Y. H. Geerts and S. Sergeyev, *Chem. Mater.*, 2009, **21**, 2789-2797.

2 H. Li, S. S. Babu, S. T. Turner, D. Neher, M. J. Hollamby, T. Seki, S. Yagai, Y. Deguchi, H. Möhwald and T. Nakanishi, *J. Mater. Chem. C*, 2013, **1**, 1943-1951.

3 P. Duan, N. Yanai and N. Kimizuka, *J. Am. Chem. Soc.*, 2013, **135**, 19056-19059.